Sodium-dependent potassium channels of a Slack-like subtype contribute to the slow afterhyperpolarization in lamprey spinal neurons

Peter Wallén[1,2], Brita Robertson[1,2], Lorenzo Cangiano[1,2], Peter Löw[2], Arin Bhattacharjee[3], Leonard K. Kaczmarek[4] and Sten Grillner[1,2]

[1]*Nobel Institute for Neurophysiology, Karolinska Institutet, Stockholm, Sweden*
[2]*Department of Neuroscience, Karolinska Institutet, Stockholm, Sweden*
[3]*Department Pharmacology & Toxicology, SUNY, Buffalo, NY, USA*
[4]*Department of Pharmacology, Yale University School of Medicine, New Haven, CT, USA*

The slow afterhyperpolarization (sAHP) following the action potential is the main determinant of spike frequency regulation. The sAHP after single action potentials in neurons of the lamprey locomotor network is largely due to calcium-dependent K^+ channels (80%), activated by calcium entering the cell during the spike. The residual (20%) component becomes prominent during high level activity (50% of the sAHP). It is not Ca^{2+} dependent, has a reversal potential like that of potassium, and is not affected by chloride injection. It is not due to rapid activation of Na^+/K^+-ATPase. This non-K_{Ca}-sAHP is reduced markedly in amplitude when sodium ions are replaced by lithium ions, and is thus sodium dependent. Quinidine also blocks this sAHP component, further indicating an involvement of sodium-dependent potassium channels (K_{Na}). Modulators tested do not influence the K_{Na}-sAHP amplitude. Immunofluorescence labelling with an anti-Slack antibody revealed distinct immunoreactivity of medium-sized and large neurons in the grey matter of the lamprey spinal cord, suggesting the presence of a Slack-like subtype of K_{Na} channel. The results strongly indicate that a K_{Na} potassium current contributes importantly to the sAHP and thereby to neuronal frequency regulation during high level burst activity as during locomotion. This is, to our knowledge, the first demonstration of a functional role for the Slack gene in contributing to the slow AHP.

The afterhyperpolarization (AHP) following each action potential is a main determinant of spike frequency and its adaptation (Kernell, 1965; Schwindt & Calvin, 1973; Gustafsson, 1974; Madison & Nicoll, 1984; El Manira *et al.* 1994; Sah & Davies, 2000). In spinal and brainstem neurons in vertebrates including the lamprey investigated here, it is composed of two components, a fast AHP accompanying the rapid repolarization due to voltage-dependent K^+ channels, followed by a slower AHP (sAHP), lasting in the order of 100 ms, due mainly to calcium-dependent, apamin-sensitive K^+ (K_{Ca}) channels (Hill *et al.* 1985, 1992; Meer & Buchanan, 1992; Cangiano *et al.* 2002). K_{Ca} channels in lamprey neurons are activated by Ca^{2+} entry through N-type and P/Q-type (Ca_v 2.1, 2.2) calcium channels (Wikström & El Manira, 1998). In cortical neurons yet another even slower AHP, lasting over a second, is also expressed (Sah & Faber, 2002).

In networks generating rhythmic burst activity, like the spinal locomotor network in lamprey, K_{Ca} channels

contribute importantly to pattern generation through their effects on spike frequency adaptation and on the termination of plateau potentials (El Manira *et al.* 1994; see Grillner, 2003). Activity-dependent changes resulting in a hyperpolarization are thus to a large extent mediated by the increase in Ca^{2+} levels near the cell membrane and the resulting activation of K_{Ca} channels. The channels underlying the sAHP are indirectly the target for several different modulatory systems, intrinsic to the spinal cord, notably the 5-HT, GABA and dopamine systems through their action on Ca^{2+} channels (Wallén *et al.* 1989*a*; Matsushima *et al.* 1993; Schotland *et al.* 1995; Hill *et al.* 2003). This modulatory influence results in an increased firing rate in response to a given excitatory input, and a less pronounced spike frequency adaptation (Wallén *et al.* 1989*a*).

We have recently shown that K_{Ca} channels only account for 80% of the sAHP following a single action potential in lamprey neurons (Cangiano *et al.* 2002). The remainder

is not dependent on Ca^{2+} entry. In this study we explore the potential role of Na^+ activated K^+ channels (K_{Na}) for the sAHP in neurons of the lamprey locomotor network. K_{Na} channels (Dryer, 1994; Bhattacharjee & Kaczmarek, 2005) are expressed in a variety of tissues, but their physiological function is unclear, although they have been proposed to ensure hyperpolarization during ischaemia (Dryer, 1994, 2003; Bhattacharjee *et al.* 2003; Uchino *et al.* 2003; Yuan *et al.* 2003), a longlasting depression of locomotor activity in tadpole (Dale, 1993), and to contribute to a hyperpolarization following prolonged burst activity (Safronov & Vogel, 1996; Franceschetti *et al.* 2003). A fast Na^+-activated K^+ current with an action limited to the duration of the action potential has recently been demonstrated in dissociated neurons of the larval lamprey spinal cord (Hess *et al.* 2007). Two subtypes of K_{Na} channels, Slick (Slo2.1) and Slack (Slo2.2), have recently been cloned (Yuan *et al.* 2003; Bhattacharjee *et al.* 2003).

We show here that a Slack-like subtype of K_{Na} channel contributes to the sAHP and thereby to neuronal frequency regulation, and that the K_{Na} action becomes prominent during high level activity. These results have, in part, been reported in abstract form (Wallén *et al.* 2002, 2005; Wallén & Grillner, 2003).

Methods

Ethical approval

All experimental procedures were approved by Stockholms Norra Försöksdjursetiska Nämnd, according to the Swedish regulations for the care and use of laboratory animals. After removal of the tissue, the animals were killed by decapitation while still anaesthetized.

Spinal cord in vitro preparation

Experiments were performed using the isolated preparation of the lamprey spinal cord (*Lampetra fluviatilis*). Data from a total of 74 recorded neurons of 42 animals forms the basis of this study. A spinal cord piece of 5–16 segments was dissected from a region caudal to the gills under MS-222 anaesthesia (tricaine methane sulphonate, 200 mg l^{-1}, dissolved in water; Sigma, St Louis, MO, USA). The spinal cord was isolated from the underlying notochord and placed with the ventral side up in a Sylgard-lined (Dow Corning, Midland, MI, USA), cooled experimental chamber, continuously perfused with cooled and oxygenated lamprey physiological solution via a peristaltic pump. The solution contained (mM): 138 NaCl, 2.1 KCl, 1.8 CaCl$_2$, 1.2 MgCl$_2$, 4 glucose, 2 Hepes, and was bubbled with O_2 and adjusted to pH 7.4 with NaOH. The spinal cord was pinned to the bottom of the chamber and fixed in place using a piece of fine mesh. Before microelectrode penetration, the meninx primitiva

was gently removed from a region of the ventral surface using fine forceps.

Extracellular recordings from the cut ends of one or two ventral roots were made using glass suction electrodes, connected to a differential AC amplifier (A-M Systems Inc., Sequim, WA, USA).

Intracellular recordings

Membrane potential recordings were made in current clamp mode using conventional glass microelectrodes (GC100TF; Harvard Apparatus Ltd, Edenbridge, Kent, UK) filled with 3 M KAc and 0.1 M KCl (electrode resistances were 35–70 MΩ). Recordings were made using an Axoclamp 2A intracellular amplifier (bandwidth DC–30 kHz; Axon Instruments Inc., Union City, CA, USA), and stored on a PC after A/D conversion (sampling rate 5 kHz) under software control (pCLAMP 9.0, Axon Instruments Inc.). To facilitate accurate measurement of the membrane potential during DC injection, the discontinuous current clamp (DCC) mode of the amplifier was used.

Neurons were stimulated to produce action potentials by intracellular current injection, using a variety of stimulus protocols like single and trains of brief (2 ms) depolarizing pulses, as well as long (1 s) depolarizing pulses for analysis of spike frequency adaptation properties. A programmable pulse stimulator unit (Master-8, A.M.P.I., Jerusalem, Israel) was used to set and deliver stimulus protocols.

Ion substitutions and drug applications

In most cases of drug application, and for all ion substitution experiments, the composition of the perfusion solution was manipulated. To study the non-calcium slow afterhyperpolarization (non-K_{Ca}-sAHP) in isolation from the calcium-dependent component of the AHP (K_{Ca}-AHP), the high-threshold (HVA) calcium channel blocker cadmium was added to the perfusion solution (CdCl$_2$, 200 μM), in some cases in combination with the low-threshold (LVA) calcium channel blocker nickel (NiCl$_2$, 200 μM). The K_{Ca}-AHP was fully blocked both in cadmium alone and in cadmium combined with nickel.

To test for a sodium dependence of the non-K_{Ca}-sAHP, a physiological solution in which sodium ions had been completely replaced by lithium ions was used. This treatment did not alter the spike initiation threshold in any appreciable way. To test for a potassium dependence of the non-K_{Ca}-sAHP, the potassium ion concentration of the normal physiological solution was increased to 5.0 mM. To further test for a possible dependence on chloride ions of the non-K_{Ca}-sAHP, chloride ions were injected intracellularly from a KCl-containing microelectrode by

negative DC injection. The capability of such a treatment to reverse the hyperpolarizing response to glycine was tested in the same cell by local pressure ejection of glycine from a broken glass pipette (1.0 mm in pipette) close to the recorded cell.

The nature of the non-K_{Ca}-sAHP was further investigated by bath application of the potassium channel blockers catechol (selectively blocks the transient K^+ current; 100 μM) and tetraethylammonium (TEA; blocks the delayed rectifier current; 200 μM), and by bath application of the K_{Na}-channel blocker quinidine (1 mm). The possible involvement of the sodium–potassium pump was tested by bath application of the Na^+/K^+-ATPase inhibitor ouabain (20 μM).

The possible influence on the non-K_{Ca}-sAHP by different modulatory systems intrinsic to the lamprey spinal cord was investigated by local pressure ejection of the receptor agonists 5-HT (10 mm in pipette) and baclofen (GABA$_B$-receptor agonist; 10 mm in pipette), and by bath application of dopamine (50 μM) and the broad-spectrum metabotropic glutamate receptor (mGluR) agonist (1S,3R)-1-aminocyclopentane-1,3-dicarboxylic acid ((1S,3R)-ACPD; 100 μM).

Glycine, catechol, TEA, quinidine, ouabain, 5-HT, baclofen and dopamine were obtained from Sigma (St Louis, MO, USA), while (1S,3R)-ACPD was obtained from Tocris (Bristol, UK).

Analysis of the slow afterhyperpolarization (sAHP)

The effects on the amplitude of the sAHP were analysed using pCLAMP software (Clampfit; Axon Instruments Inc.). The sAHP amplitude was measured in relation to the baseline membrane potential level immediately preceding the stimulus pulse. The amplitude of the summed sAHP following a train of stimulus pulses was measured relative to the baseline membrane potential level preceding the first pulse. In general, the average amplitude of the sAHP following at least 30 stimuli (single pulses or trains) was calculated.

Immunohistochemistry

In order to link the presence of the Slack protein to neurons with a slow K_{Na}-AHP, recorded neurons were intracellularly labelled with neurobiotin ($n = 5$). The spinal cord was then fixed in 4% formalin and 14% saturated picric acid in 0.1 M phosphate buffer (PB) for 4–12 h. After 24 h in 20% sucrose, 20 μm cryostat sections were cut and incubated with a rabbit anti-Slack antibody (0.5 μg ml^{-1}), targeting the C-terminal of Slack. The neurobiotin was visualized with Cy2-streptavidin (1 : 1000; Jackson Immunoresearch, West Grove, PA, USA) and the Slack antibody with a donkey anti-rabbit IgG-Cy3

(1 : 500; Jackson Immunoresearch). Two other antibodies, raised in chicken, were also tested: anti-Slack B and anti-Slick. None of these gave, however, any specific labelling in lamprey spinal cord tissue.

As control, the anti-Slack antibody (0.5 μg ml^{-1}) was preabsorbed with the antigenic peptide KA1628 (5 μg ml^{-1}; a 20 amino acid peptide with the sequence: free-GCDVMNRVNLGYLQDEMNDH-COOH). The antibody/peptide solution was heated for 30 min at 37°C and centrifuged, and the supernatant was applied to spinal cord sections as described above. For comparison, additional sections were incubated with the anti-Slack antibody treated the same way (heating and centrifugation) as the preabsorbed antibody. Some spinal cord sections were also incubated with the non-treated anti-Slack antibody.

Western blots

Protein extracts from lamprey and rat brains were subjected to gel electrophoresis on NUPAGE-Mops 4–12% gradient gels (Invitrogen, Carlsbad, CA, USA) and subsequently transferred to PVDF membranes. Western blots were developed with Immobilon Western (Millipore Corporation, Billerica, MA, USA).

Results

A total of 51 lamprey spinal cord grey matter neurons were subjected to a detailed analysis in this study. The cells had a mean resting membrane potential (V_m) of -70.7 mV (± 4.7 mV, s.d.) and a mean action potential amplitude of 91.2 mV (± 7.3 mV, s.d.). Sixteen cells were motoneurons, identified by monitoring the unit spike in a ventral root. No significant differences with regard to the slow AHP were seen between results obtained from motoneurons and those from other grey matter neurons.

A non-K_{Ca}-dependent component of the slow AHP

The slow AHP (sAHP) evoked in motoneurons after a single action potential is largely due to K_{Ca} channels activated by Ca^{2+} entry during the action potential. They are apamin sensitive (Hill *et al.* 1992; Meer & Buchanan, 1992; Cangiano *et al.* 2002). Under control conditions in the present study, the mean amplitude of the sAHP following a single action potential was 2.7 mV (± 0.6 mV, s.d., $n = 17$ cells). After a blockade of Ca^{2+} entry by Cd^{2+}, a small component remains (20.7% of the control sAHP ± 7.6%, s.d.), as shown in Fig. 1Aa (see Cangiano *et al.* 2002). When instead of a single action potential a high-frequency train was given with increasing number of spikes, this Ca^{2+}-independent component grew progressively, and more so than the

control sAHP (Fig. 1*A* and *B*). The relative contribution of the non-K_{Ca}-dependent component (the non-K_{Ca}-sAHP) was further analysed in five cells, and represented 43.6% ($\pm4.1\%$, s.e.m.) of the control sAHP after 10 action potentials (Fig. 1*C*), and with even longer stimulus trains the non-K_{Ca}-sAHP grew to more than 50%. This marked incremental effect on the non-K_{Ca}-sAHP by train stimulation with increasing number of spikes was found in all of nine cells tested (five of which were motoneurons).

The non-K_{Ca}-dependent component of the sAHP is thus clearly dependent on the activity level. Its amplitude also increases markedly with increasing spike frequency (Fig. 2). In three cells the relative contribution of the non-K_{Ca}-sAHP was further analysed, and found to increase from 19.2 to 44.1% of the control sAHP when the frequency was increased from 20 to 100 Hz in a train of 10 spikes (Fig. 2*C*). These spike rates are within the physiological range for motoneuronal firing in lamprey

(Wallén *et al.* 1989*a*; Buchanan, 1993; Martin, 2002). The non-K_{Ca}-sAHP increased progressively with frequency, whereas the K_{Ca} component saturated early (Fig. 2*B*). The incremental effect on the non-K_{Ca}-sAHP by train stimulation with increasing frequency of spikes was found in all of seven cells tested (two of which were motoneurons).

The non-K_{Ca}-sAHP is Na$^+$ dependent

What mechanism could be responsible for the non-K_{Ca}-sAHP? Because it persists in the presence of Cd^{2+}, and also after intracellular injection of BAPTA and after blockade of K_{Ca} channels by apamin (Cangiano *et al.* 2002), a calcium-dependent mechanism may be excluded. To explore the possibility that sodium-dependent potassium channels (K_{Na} channels; Dryer, 1994, 2003) may be involved, we first replaced sodium with lithium,
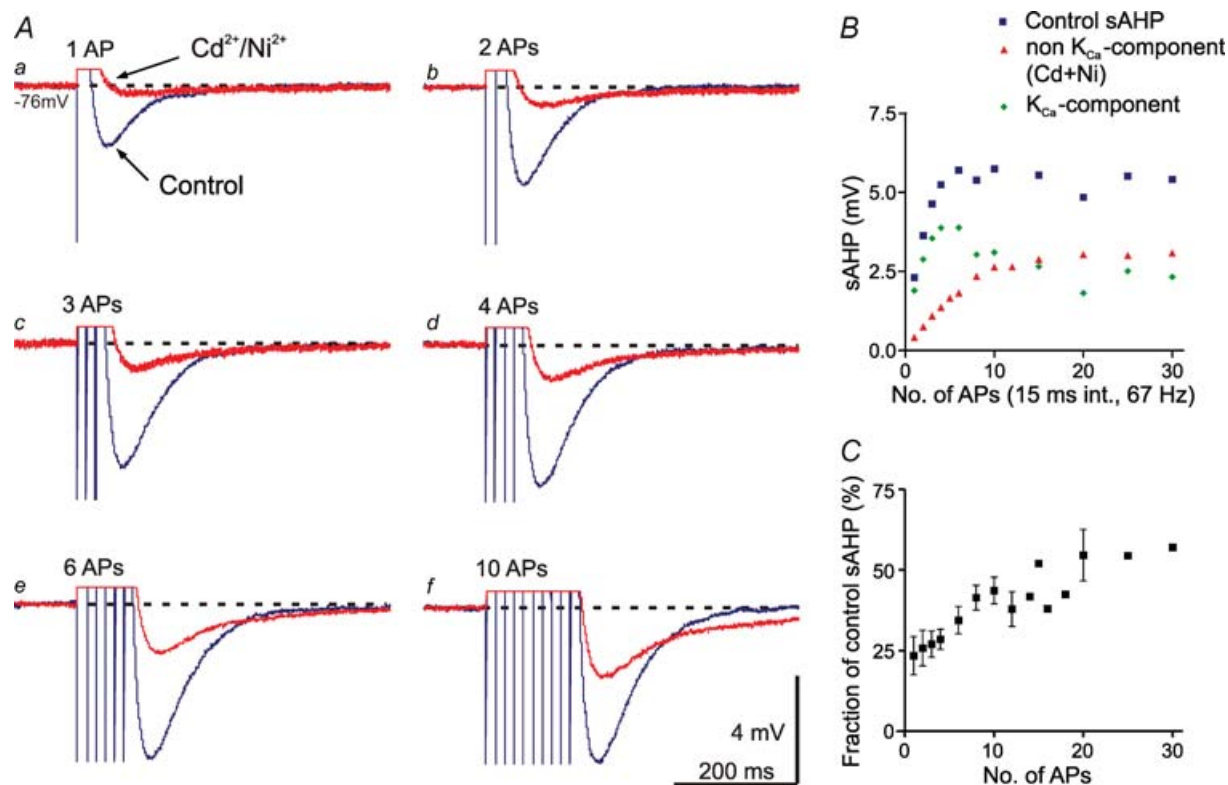

Figure 1. Summation of the sAHP with increasing number of action potentials
A, with increasing number of action potentials (APs) elicited in the pulse train (*a–f*; 15 ms interval), there was a marked increase in amplitude of the control sAHP (blue traces), as well as of the non-K_{Ca}-sAHP (red traces) recorded in the presence of Cd^{2+} (200 μM) and Ni^{2+} (200 μM). The non-K_{Ca} component grew progressively more. Dotted lines indicate membrane potential level before onset of stimulation. AHP traces in this and subsequent figures are averages of at least 30 individual trials. Scale bars in *Af* apply to all traces. *B*, dependence of the sAHP amplitude (ordinate; mean values of 30 or more stimulus sweeps) on the number of action potentials in the train. The control sAHP (blue squares) grew to a maximum of about 5 mV already after four spikes, while the non-K_{Ca}-sAHP (red triangles) reached its maximum after about 10 spikes. Data from the same grey matter neuron are illustrated in *A* and *B*, V_{m} was -76 mV. *C*, data summarized from five cells, illustrating the increase of the relative contribution of the non-K_{Ca} component to the sAHP with increasing number of action potentials, plotted as fraction (%) of the control sAHP (means $\pm$ s.e.m.).

an ion species that also passes through Na^+ channels and generates an action potential, but does not activate K_{Na} channels (Safronov & Vogel, 1996; Bischoff *et al.* 1998). In Li^+ the non-K_{Ca}-sAHP was markedly depressed (Fig. 3*A*). Following reintroduction of Na^+, an almost complete recovery was seen (Fig. 3*Aa*). While the non-K_{Ca}-sAHP was reduced in Li^+, the action potential area remained unaltered (Fig. 3*Ab*; see below, Fig. 4). A clear reduction of the non-K_{Ca}-sAHP in Li^+ was seen in all of six tested neurons, with a significant mean reduction of 63.6% (±7.2%, s.e.m., $P < 0.001$, one-sample *t* test). The fact that the non-K_{Ca}-sAHP was not completely abolished in Li^+ is likely to be due to incomplete washout of Na^+ during the experiment. These results show that Na^+ entry is required to evoke the non-K_{Ca}-sAHP, possibly through the activation of K_{Na} channels. Sodium substitution also depressed the initial fast AHP. This effect is presumably due to a reduction of a transiently activated, fast K_{Na} current, suggested to contribute to the early repolarization of the action potential (Hess *et al.* 2007). This fast K_{Na} current is

thus separate from the Na^+-dependent current underlying the non-K_{Ca}-sAHP.

The non-K_{Ca}-sAHP current is carried by K^+ but not Cl^-

We next investigated whether the hyperpolarizing current during the non-K_{Ca}-sAHP is carried by Cl^- or K^+ ions. To test the former case, we compared the amplitude of the non-K_{Ca}-sAHP before and after injecting Cl^- ions through the microelectrode. No modification of the non-K_{Ca}-sAHP was observed (Fig. 3*Ba*; $n = 3$ cells of which 2 were motoneurons). To confirm that the Cl^- equilibrium potential had been changed, a small extracellular 'puff' of glycine was administered to the same cell before and after the Cl^- injection (Fig. 3*Bb*). The initial hyperpolarization was reversed to a depolarization after Cl^- injection, in the case illustrated even evoking a few action potentials (truncated in Fig. 3*Bb*), demonstrating a shift of the Cl^- equilibrium potential. Cl^- ions thus do not contribute to the non-K_{Ca}-sAHP. Since the reversal potential of the
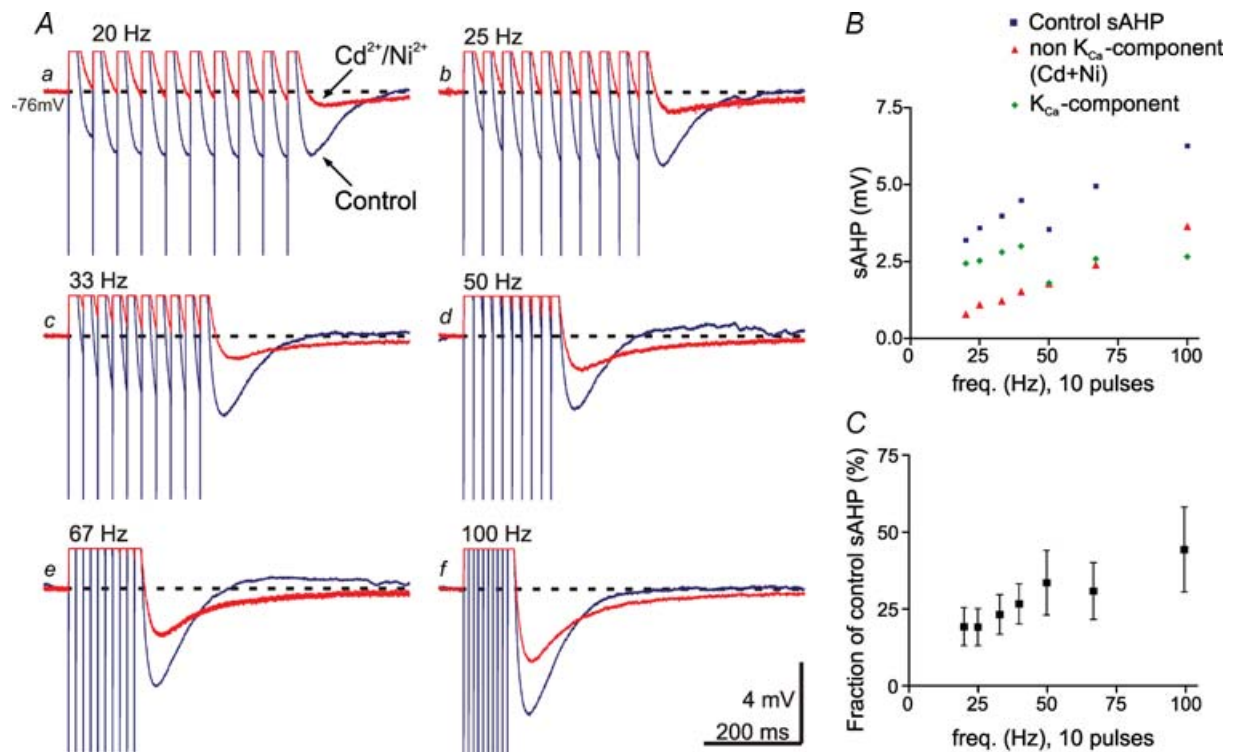

Figure 2. Summation of the sAHP with increasing frequency of action potentials
A, with increasing frequency of action potentials (APs) elicited in the pulse train (*a–f*; 10 pulses), there was a marked increase in amplitude of the control sAHP (blue traces), as well as of the non-K_{Ca}-sAHP (red traces) recorded in the presence of Cd^{2+} (200 μM) and Ni^{2+} (200 μM). Dotted lines indicate membrane potential level before onset of stimulation. Scale bars in *Af* apply to all traces. *B*, dependence of the sAHP amplitude (ordinate; mean values of 30 or more stimulus sweeps) on the frequency of action potentials in the train. The non-K_{Ca}-sAHP (red triangles) grew progressively more than the control sAHP (blue squares). Data from the same grey matter neuron is illustrated in *A* and *B*; V_m was -76 mV (same cell as in Fig. 1*A* and *B*). *C*, data summarized from three cells, illustrating the increase of the relative contribution of the non-K_{Ca} component to the sAHP with increasing frequency of action potentials, plotted as fraction (%) of the control sAHP (means ± s.e.m.).

non-K_{Ca}-sAHP is the same as that of K^+ (see below, Fig. 5), the remaining possibility would be that the underlying current is a potassium current. In confirmation of this, when the extracellular K^+ concentration was changed from 2.1 to 5 mM, the amplitude of the non-K_{Ca}-sAHP was markedly reduced (by 29.3 and 60.8%, respectively, in two cells tested), as anticipated from the accompanying reduction in the K^+ equilibrium potential (Fig. 3C). The non-K_{Ca}-sAHP current thus appears to be carried by K^+, as is the larger K_{Ca} component.

Effects of K^+ channel blockers on the non-K_{Ca}-sAHP

An important part of the repolarization of the action potential is due to activation of a fast transient K^+ current and delayed rectifiers also contribute (Hess & El Manira,

2001; Lamotte d'Incamps *et al.* 2004). The former current is selectively blocked by catechol at 100 μM, and the latter is blocked by a low concentration of the general blocker tetraethyl ammonium (TEA, 200 μM). We next tested whether these K^+ channel blockers would also block the K^+ current underlying the non-K_{Ca}-sAHP. Both catechol and TEA (Fig. 4) caused a marked broadening of the action potential, but also an enhancement of the non-K_{Ca}-sAHP, rather than a blockade. The progressive increase in amplitude of the non-K_{Ca}-sAHP was evident after a single action potential (Fig. 4A and D), as well as after a spike train (Fig. 4B and E). This effect on the non-K_{Ca}-sAHP was seen in all of five tested cells, with a significant mean amplitude increase of 138.7% ($\pm$31.4%, S.E.M., $P < 0.05$, one-sample t test). The spike broadening increases the area under the action potential due to the
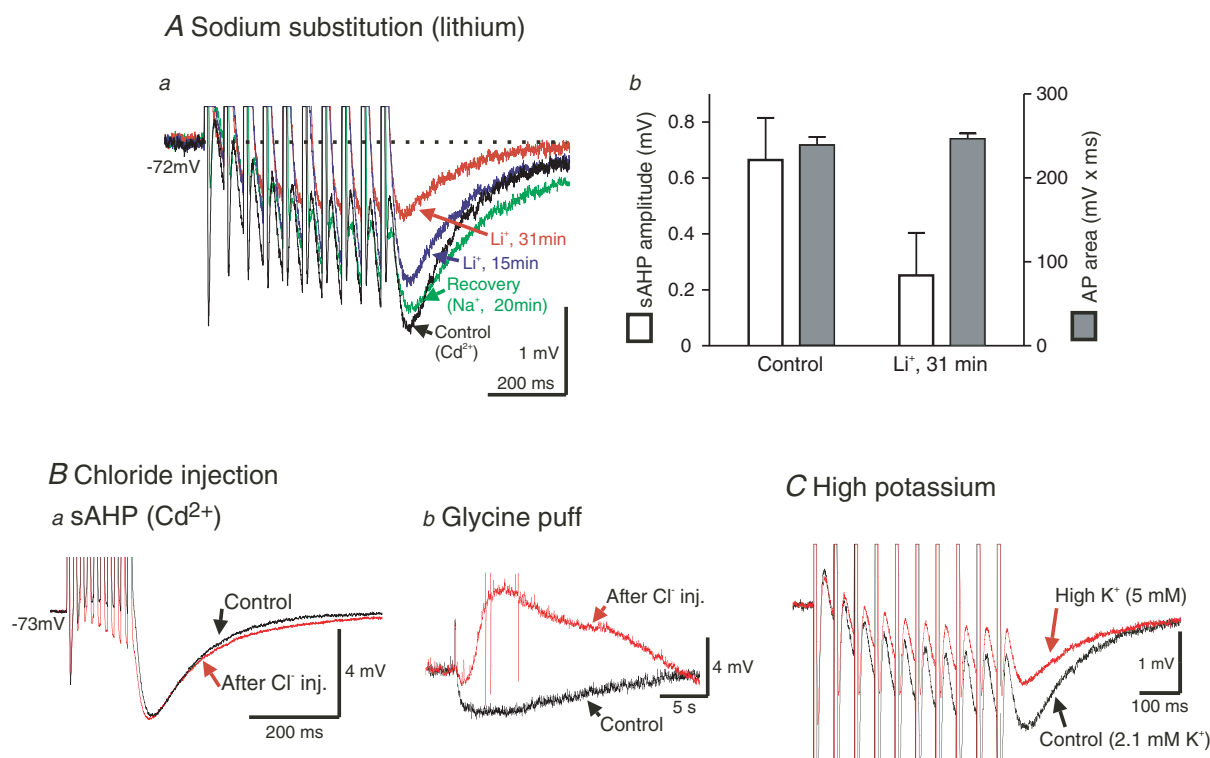

Figure 3. The non-K_{Ca}-sAHP is caused by a sodium-dependent potassium current
A, when Na^+ ions were completely replaced with Li^+ ions, the non-K_{Ca}-sAHP progressively diminished in amplitude with time after start of bath perfusion with Li^+-containing physiological solution. *Aa*, in Li^+, the non-K_{Ca}-sAHP following a train of 10 action potentials was reduced (by 51% in this cell; 200 μM Cd^{2+} present throughout experiment). Almost complete recovery was achieved at 20 min after Na^+ reintroduction in this case. *Ab*, the amplitude of the non-K_{Ca}-sAHP following a single action potential (left ordinate, mean values $\pm$ S.D., $n = 42$ stimulus sweeps) was reduced in lithium without any significant change of the action potential area (right ordinate, mean values $\pm$ S.D., $n = 42$ stimulus sweeps). Same grey matter neuron in *Aa* and *b*, V_m was -72 mV. *B*, intracellular injection of Cl^- ions had no effect on the non-K_{Ca}-sAHP. *Ba*, a summed non-K_{Ca}-sAHP was evoked by train stimulation in the presence of Cd^{2+} (control, black trace). After Cl^- injection from the microelectrode no apparent change of the non-K_{Ca}-sAHP occurred (red trace). *Bb*, in the same cell as in *a* (motoneuron, V_m was -73 mV), the efficacy of the Cl^- injection in shifting the Cl^- equilibrium potential was checked by local, extracellular application of glycine from a pressure pipette, demonstrating clear reversal of the response. *C*, increasing the extracellular K^+ concentration from 2.1 (Control) to 5 mM (red trace) reduced the size of the non-K_{Ca}-sAHP (Cd^{2+} present; grey matter neuron, V_m was -62 mV with some depolarization (approximately 9 mV) occurring in high K^+).

blockage of K$^+$ currents. As further illustrated for the cells in Fig. 4, the increase in amplitude of the non-K_{Ca}-sAHP occurred in parallel with the increase in action potential area (Fig. 4*C* and *F*). The non-K_{Ca}-component of the sAHP is thus clearly not due to TEA- or catechol-sensitive K$^+$ channels.

The sodium–potassium pump and the non-K_{Ca}-sAHP

The sodium–potassium pump (Na$^+$/K$^+$-ATPase), which maintains the K$^+$ equilibrium potential, is continuously active and is dynamically regulated by intracellular Na$^+$ levels. The possibility that the non-K_{Ca}-sAHP is due to a dynamic activation of the Na$^+$/K$^+$-ATPase should also be considered, since the pump is electrogenic, and enhanced activity would cause a hyperpolarization. To explore this possibility, we tested the effect of inhibiting the pump with ouabain (20 μM) in five neurons. Ouabain indeed affected the non-K_{Ca}-sAHP, which decreased markedly with time, and even reversed (Fig. 5*A*, records taken at −65 mV membrane potential). An inhibition of the pump leads to a

progressive reduction of the equilibrium potential for K$^+$, which in turn results in a change in the reversal potential for the non-K_{Ca}-sAHP. Figure 5*B* shows that the sAHP reversal potential (green symbols; mean $\pm$ s.d., $n = 30$ train stimuli; same cell as in *A*), determined by eliciting the sAHP at a range of membrane potential holding levels at different time points during ouabain application, changed in parallel with both the resting membrane potential (black symbols) and the amplitude of the non-K_{Ca}-sAHP (red symbols; here measured at −65 mV at all time points). In all five cells tested (including two motoneurons), the decrease of the amplitude of the non-K_{Ca}-sAHP in ouabain was accompanied by a change of the sAHP reversal potential and the resting membrane potential. Figure 5*C* illustrates the dependence of the non-K_{Ca}-sAHP amplitude on the sAHP reversal potential.

The maintenance of a non-K_{Ca}-sAHP during blockade of the Na$^+$/K$^+$-ATPase could be demonstrated by depolarizing the neuron above the reversal potential at different times during the ouabain application. Figure 5*D* shows the uncovered sAHP (red traces) at three time points
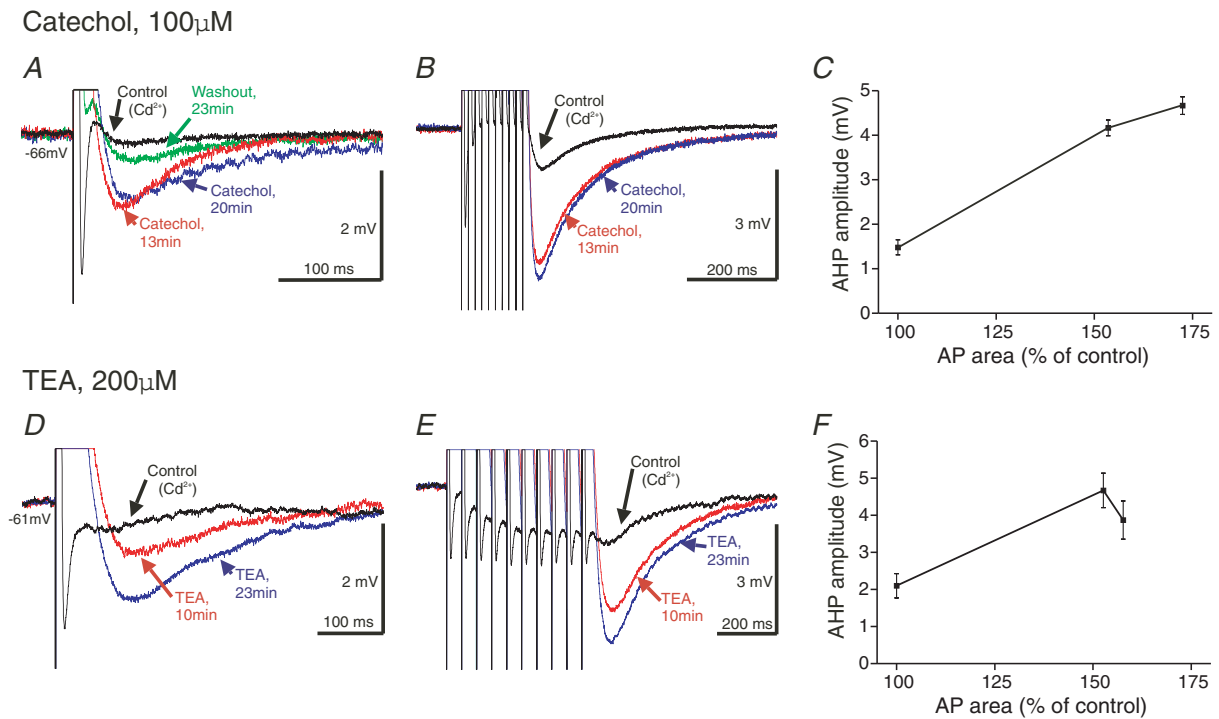

Figure 4. The non-K_{Ca}-sAHP is not blocked by the K$^+$ channel blockers catechol and TEA
A–C, effects of catechol (100 μM, bath application). In *A* it is shown that the non-K_{Ca}-sAHP following a single spike is not reduced, but rather increased, in amplitude with time after the start of catechol-perfusion. The fast AHP is abolished and the spike becomes broader in catechol. *B*, the increase in amplitude of the summed non-K_{Ca}-sAHP following catechol application (215% increase after 20 min in this cell). *C*, the parallel increase of the action potential area (abscissa; expressed as percentage of the control value) and the increase in the non-K_{Ca}-sAHP amplitude (ordinate; mean $\pm$ s.d., $n = 29$ or more stimulus sweeps), following catechol administration. Same grey matter neuron in *A–C*, V_m was −66 mV. *D–F*, effects of tetraethyl ammonium (TEA; 200 μM, bath application). The corresponding effects as found with catechol were also seen with TEA application. Same grey matter neuron in *D–F*, V_m was −61 mV.

during ouabain (same cell as in Fig. 5*A–C*). The amplitude of the uncovered sAHP decreased with time as the cell was more depolarized, which also caused the amplitude of the corresponding action potentials to decrease (Fig. 5*Dd*). The sAHP can thus still be revealed during blockade of the pump, and the decrease of its amplitude may be explained by the concomitant change of the sAHP reversal potential. The non-K_{Ca}-sAHP can therefore not be accounted for by a dynamic activation of the Na^+/K^+-ATPase.

The effect of quinidine on the non-K_{Ca}-sAHP

Taken together, the present findings indicate that sodium-activated potassium channels, K_{Na} channels (Dryer, 1994, 2003; Bhattacharjee & Kaczmarek, 2005), are responsible for the non-K_{Ca}-sAHP in spinal lamprey

neurons. The cardiac antiarrhythmic drug quinidine has been reported to effectively block the two cloned subtypes of K_{Na} channels, Slick (Slo2.1) and Slack (Slo2.2) (Bhattacharjee *et al.* 2003). We therefore tested the effect of quinidine (1 mM). In all of four cells tested, and as illustrated in Fig. 6*A*, application of quinidine markedly reduced the amplitude of the non-K_{Ca}-sAHP (red trace in Fig. 6*Aa*), with a significant mean reduction of 43.0% ($\pm$7.9%, s.e.m., $P < 0.05$, one-sample t test). In doing so, quinidine did not significantly affect the shape of the action potential (Fig. 6*Ab*). While quinidine did not cause complete abolition of the non-K_{Ca}-sAHP, presumably due to incomplete block during the course of application, these results provide further evidence for an involvement of K_{Na} channels in the generation of the non-K_{Ca}-sAHP. Quinidine does not, however, allow discrimination between the Slick and Slack subtypes of K_{Na} channels.
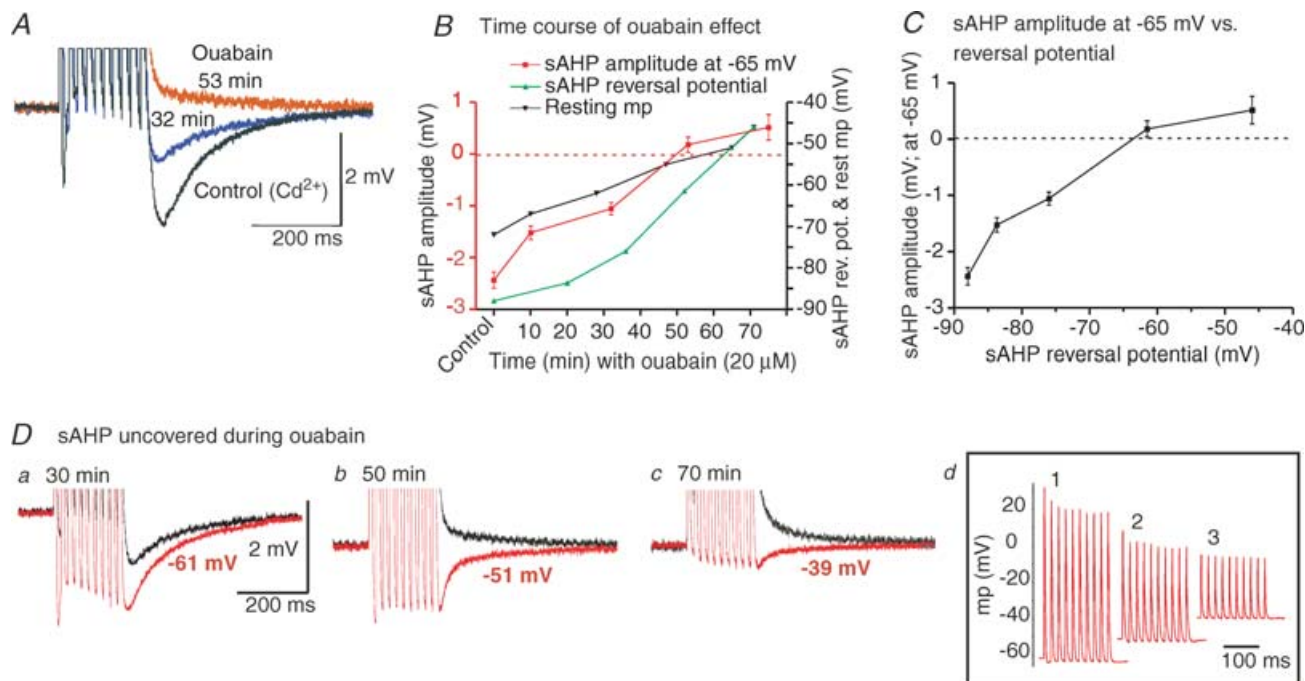

Figure 5. Effects of Na^+/K^+ pump inhibition on the non-K_{Ca}-sAHP
A, comparison of the non-K_{Ca}-sAHP in control conditions (200 μM Cd^{2+} present), and after bath application of the Na^+/K^+ ATPase inhibitor ouabain (20 μM). The membrane potential was kept at -65 mV by DC injection in all three trials illustrated. There was a marked reduction and even reversal of the non-K_{Ca}-sAHP in ouabain. *B*, time course of the effects of Na^+/K^+ pump inhibition. In the presence of ouabain the non-K_{Ca}-sAHP, here measured at -65 mV, decreased in amplitude over time and reversed to a depolarization after about 50 min (red curve, left ordinate). The reversal potential of the non-K_{Ca}-sAHP was determined by amplitude measurements at a range of membrane potential holding levels at each time point during ouabain application. The non-K_{Ca}-sAHP reversal potential (green curve, right ordinate) decreased from -88 mV at control to -46 mV at the end of the experiment, and paralleled the decrease in the non-K_{Ca}-sAHP amplitude. A concomitant decrease of the resting membrane potential level was also evident (black curve, right ordinate). *C* illustrates the relation between the reversal potential of the non-K_{Ca}-sAHP and its amplitude (measured at -65 mV). Values plotted in *B* and *C* are means $\pm$ s.d., $n = 30$ or more stimulus sweeps. *D*, a maintained non-K_{Ca}-sAHP could be uncovered during ouabain application. Depolarizing the neuron above the reversal potential revealed a hyperpolarizing non-K_{Ca}-sAHP at different time points (*a–c*; red traces, holding potential levels indicated). Black traces show the sAHP at -65 mV. In *d* are shown the corresponding action potential trains at the three time points in *a–c*. Same grey matter neuron in *A–D*, resting V_m was -73 mV.

Immunohistochemistry using an anti-Slack antibody

We next explored the presence of K_{Na} channels in lamprey neurons using immunohistochemistry. Immuno-fluorescence labelling with an anti-Slack antibody revealed distinct expression of the Slack protein in medium-sized and large neurons in the grey matter of the lamprey spinal cord, both in their somata and in their dendrites (Fig. 6*C*). The size and location of the labelled cells suggest that they include motoneurons as well as network interneurons. The labelling appeared highly selective, since no labelling of, for example, some small cells, the dorsal column, or the large reticulospinal axons was detected.

In control experiments, incubation of spinal cord sections with the anti-Slack antibody preabsorbed with the antigenic peptide (see Methods) completely abolished all immunostaining (not illustrated), whereas the anti-Slack antibody treated the same way as the preabsorbed antibody gave identical immunostaining to the one that received no heat and centrifugation treatment. This control finding further supports the notion that the Slack labelling was specific in the lamprey spinal cord. A Slick antibody, raised in chicken (Bhattacharjee *et al.* 2005), failed to give specific labelling in the lamprey spinal cord.

In order to link the presence of the Slack protein to neurons with a slow K_{Na}-AHP, recorded neurons were
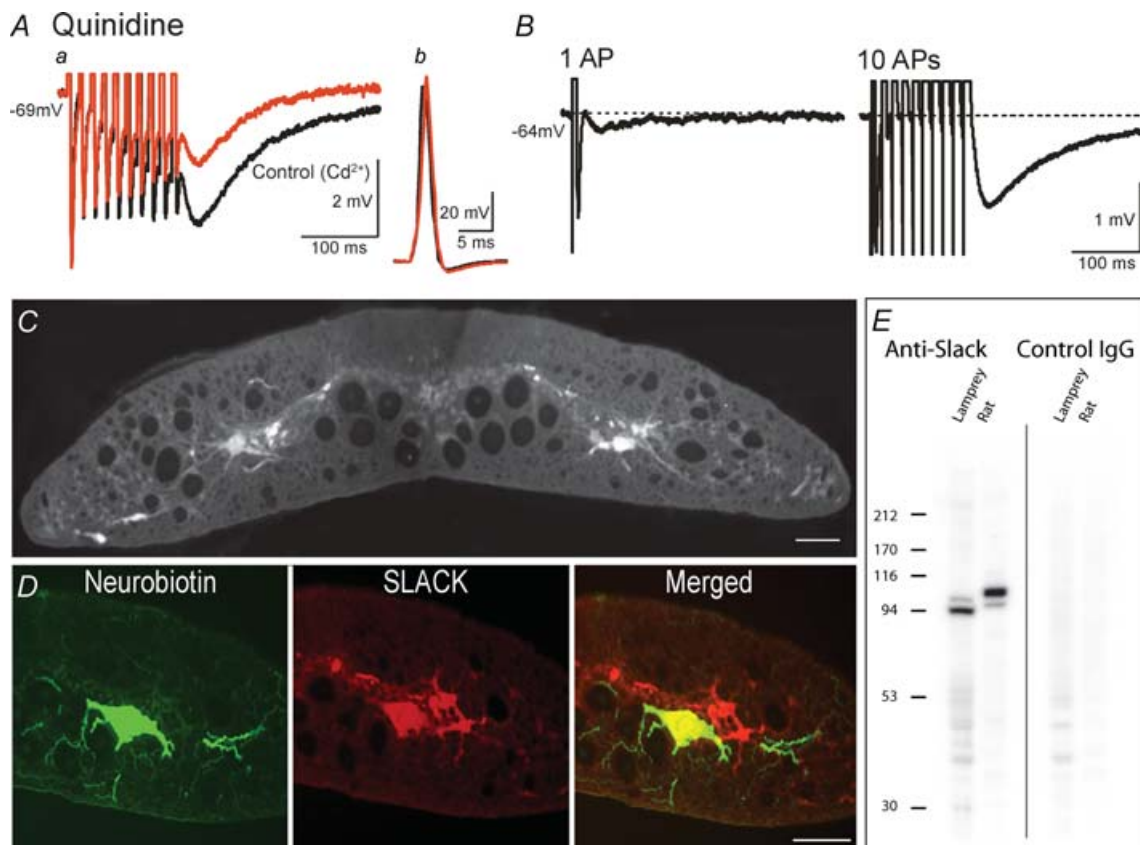

Figure 6. The effect of quinidine on the non-K_{Ca}-sAHP, and immunohistochemical evidence for a Slack-like subtype of K_{Na} channel in the lamprey spinal cord
A, quinidine blocks the two cloned subtypes of K_{Na} channels, Slick (Slo2.1) and Slack (Slo2.2) (Bhattacharjee *et al.* 2003), and when bath applied to the lamprey spinal cord, quinidine (1 mM) markedly reduced the non-K_{Ca}-sAHP (*Aa*, red trace; reduction by 45% in this cell). At the same time, the action potential remained largely unaffected (*Ab*, black trace – control, red trace – quinidine). Grey matter neuron, V_m was −69 mV. *B*, the non-K_{Ca}-sAHP (cadmium present) following a single spike and after a spike train, recorded in a grey matter neuron (V_m was −64 mV) that was then labelled by neurobiotin injection from the microelectrode (*D*, green, left panel). *C*, immuno-fluorescence labelling with a Slack antibody revealed distinct expression of the Slack protein in neurons in the grey matter of the lamprey spinal cord, both in their somata and in their dendrites. *D*, immunohistochemistry of sections of the spinal cord in which the neuron in *B* was recorded, revealing expression of the Slack protein in the same cell, primarily in the soma and proximal dendrites (red, middle panel). The right panel shows the combined image, with double labelling of the cell (yellow). Scale bars in *C* and *D* correspond to 50 μm. *E*, Western blot experiment, confirming the presence of a Slack protein in lamprey. A major band around 100 kDa was evident in lamprey brains, which is in the range of where the rat Slack protein migrates on these gels (see Methods).

intracellularly injected with neurobiotin, allowing the combined visualization of neurobiotin labelling and Slack immunohistochemistry. The neuron in Fig. 6D had a clear, slow K_{Na}-AHP following a single spike, increasing in amplitude after a spike train (Fig. 6B; cadmium present). After recording, the cell was labelled by neurobiotin (Fig. 6D; green, left panel). Immuno- histochemistry of sections of the whole-mount revealed expression of the Slack protein in the same cell, primarily in the soma and proximal dendrites (Fig. 6D; red, middle panel). The right panel in Fig. 6D shows the combined image, with double labelling of the cell (yellow). The cell thus expressed the Slack protein. The presence of a slow K_{Na}-AHP and the Slack protein was seen in 4 out of 5 tested grey matter neurons in the lamprey spinal cord. The fifth cell did not display the typical slow AHP and did not express the Slack protein (not illustrated). These findings thus suggest that a Slack-like subtype of K_{Na} channel is present in cells that exhibit the slow K_{Na}-AHP in lamprey spinal neurons.

To further corroborate the immunohistochemical findings of a Slack protein in lamprey neurons, immuno- blot experiments were also performed. As illustrated in Fig. 6E, Western blot showed a major band around 100 kDa in lamprey brains, which is in the range of where the rat Slack protein migrates on these gels, thus confirming the presence of Slack in the lamprey CNS.

Spike frequency regulation through the sAHP and the K_{Na} component

How is spike frequency regulation in the neuron influenced after blockade of the K_{Ca}-sAHP, i.e. what are the firing properties under conditions when the K_{Na} component of the sAHP is present and operating without the K_{Ca} component?

Figure 7Aa and b shows two trains of action potentials in a motoneuron, elicited during control conditions by long, depolarizing current pulses (1 s) of 0.6 nA and 1.0 nA, respectively. Figure 7Ca shows the dynamic change of spike frequency in the same cell due to summation of consecutive sAHPs during control conditions. The first interspike interval is shorter than the subsequent ones, and therefore the instantaneous spike frequency of the first interval (red symbols; mean ± s.d., $n = 20$ or more stimulus sweeps) is higher, especially at higher current amplitudes. There is therefore a powerful spike frequency adaptation. After a blockade of the K_{Ca} component, the sAHP is much smaller, manifested by a higher frequency during the current pulses of 0.6 and 1.0 nA (Fig. 7Ba and b; same cell as in Fig. 7A). A few spikes failed during the later part of the stimulus pulse at the lower strength in this example (Ba). The sAHP reduction also resulted in a smaller difference in instantaneous frequencies of the

three first interspike intervals – there was thus less spike frequency adaptation (Fig. 7Cb). In Fig. 7Cc the difference in steady-state frequency at the end of the pulse at different levels of current injection is compared, and with the K_{Ca}-sAHP blocked, the steady-state frequency is higher (red symbols). In the absence of the K_{Ca}-component of the sAHP, the cell will thus fire with a higher frequency in response to the same depolarizing input, while spike frequency adaptation is reduced but not abolished. The corresponding effects were found in all of seven cells tested, three of which were motoneurons.

The K_{Na}-sAHP contribution during burst firing

To explore the role of the sAHP and in particular the K_{Na} component during burst activity, a stimulus protocol resembling the situation occurring during activity of the locomotor network was used. The neuron was stimulated to fire four action potentials in a burst followed by a silent interval (the burst occupied approximately 40% of the cycle; Fig. 8; $n = 5$). Such bursts were delivered at a rate of 2, 5 and 8 Hz corresponding to different rates of locomotion within the natural range. With a burst frequency of 2 Hz, the control sAHP (blue trace) of the four action potentials (interval 50 ms) summed efficiently (Fig. 8Aa). The sAHP recovered to baseline during the 350 ms interburst interval. The K_{Na}-sAHP was however, very small at this burst rate (red trace; Fig. 8Ab). At the 5 Hz burst rate (20 ms interspike interval) the summation of the control sAHP was much more prominent and the recovery to baseline after the last burst took over 1 s (Fig. 8Ba), i.e. much longer than the interburst interval (140 ms; Fig. 8Bb). This resulted in a net hyperpolarization during the period of burst stimulation. The K_{Na}-sAHP contribution was now significant, but almost recovered back to baseline between bursts (Fig. 8Bb). Finally at 8 Hz burst rate (15 ms interspike interval) the K_{Na}-sAHP was substantial, and did not fully recover during the interburst interval (80 ms; Fig. 8Ca and b). This again resulted in some degree of net hyperpolarization, but much less than with the full sAHP (Fig. 8C). Corresponding results were obtained in all of five tested cells, all of which were motoneurons. The findings emphasize the important role for sAHP summation during rhythmic bursting, and furthermore demonstrate that the K_{Na} component can contribute significantly at higher burst rates.

The effects of intrinsic spinal modulator systems on the sAHP

A modulation of the amplitude of the sAHP has a powerful effect on neuronal spike frequency regulation (see Fig. 7). The K_{Ca} component is known to be markedly depressed by several transmitters like 5-HT and dopamine,

and by $GABA_B$ receptor activation (Wallén *et al.* 1989*a*; Matsushima *et al.* 1993; Schotland *et al.* 1995). We therefore investigated if these transmitters, which are intrinsic modulators in the lamprey spinal cord (Schotland *et al.* 1995; Tegnér *et al.* 1993), would also influence the K_{Na}-sAHP. This sAHP component was unaffected by administration of 5-HT (Fig. 9*Ab*; $n = 4$ cells), dopamine (Fig. 9*C*; $n = 4$ cells) or the $GABA_B$ agonist baclofen (Fig. 9*Bb*; $n = 4$ cells), whereas the control sAHP including the K_{Ca} component was markedly depressed (Fig. 9*Aa* and *Ba*), as shown previously (Wallén *et al.* 1989*a*; Matsushima *et al.* 1993; Schotland *et al.* 1995).
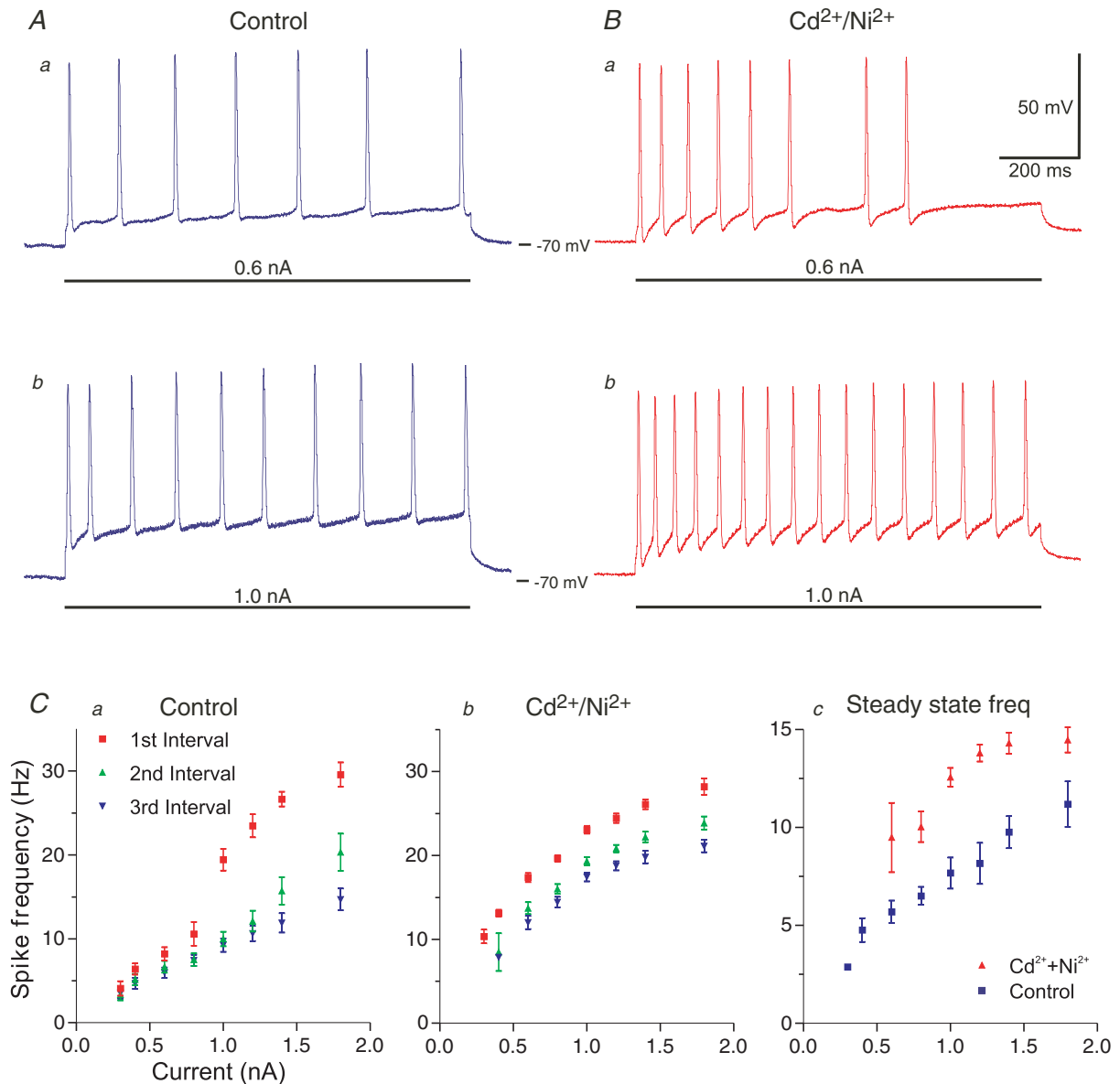

Figure 7. Spike frequency regulation and the non-K_{Ca}-sAHP
A, repetitive firing during control conditions (no Cd^{2+} present) evoked by 1 s long, depolarizing current pulses (horizontal bars) of 0.6 nA (*a*) and 1.0 nA (*b*). The higher current strength resulted in higher firing rate and substantial frequency adaptation. *B*, repetitive firing in the presence of Cd^{2+} and Ni^{2+}. Same cell as in *A* (motoneuron, V_m was −70 mV; recording was made in DCC-mode; see Methods). With only the non-K_{Ca}-sAHP operating, firing rate was higher in response to the same current. Spike frequency adaptation is still evident. Time and voltage calibration in *Ba* applies to all traces in *A*–*B*. *C*, current–frequency diagrams of repetitive firing responses to 1 s pulses, as in *A* and *B*. The instantaneous spike frequency of the first three intervals during control conditions (no Cd^{2+} present) is shown in *a*, and with only the non-K_{Ca}-sAHP operating in *b*. In *c* the steady state frequency at the end of the 1 s pulse has been plotted *versus* current strength. With only the non-K_{Ca}-sAHP operating (red symbols), the steady state frequency is enhanced. Values plotted in *Ca–c* are means ± S.D., $n = 20$ or more stimulus sweeps. Same motoneuron in *A–C*.

In addition to its fast ionotropic actions, glutamate also exerts a modulatory influence in the lamprey spinal cord via activation of metabotropic glutamate receptors (mGluRs; Krieger *et al.* 1996, 2000). mGluR1 and mGluR5 both act postsynaptically (Krieger *et al.* 2000; Kettunen *et al.* 2002, 2003) and become activated by the mGluR agonist (1*S*,3*R*)-ACPD. To explore a possible mGluR influence on the K_{Na}-sAHP, the effect of ACPD (100 μM) was also tested (Fig. 9*D*; *n* = 3 cells). There was, again, no reduction of the K_{Na}-sAHP in any of the cells tested, one of which was a motoneuron. There is thus no evidence to suggest that the K_{Na}-sAHP is subjected to modulation by any of these modulator systems, which otherwise have a prominent effect at the spinal level.

Discussion

The present study investigates the calcium-independent component of the slow AHP in lamprey spinal neurons,

its underlying mechanisms and functional significance. This non-K_{Ca}-sAHP is readily discernable even after a single action potential (see Cangiano *et al.* 2002), and it will furthermore sum very effectively during repetitive firing and even more so than the K_{Ca} component, so that after a spike train it may constitute more than half of the summed control sAHP (Figs 1 and 2). Most likely the non-K_{Ca}-sAHP will therefore play a significant role for firing properties during burst firing.

The non-calcium-dependent sAHP is due to a sodium-activated potassium current (K_{Na}), mediated by the Slack gene

The nature of the calcium-independent component of the sAHP was investigated in several steps. We first explored the possibility that the non-K_{Ca}-sAHP could be due to a sodium-dependent potassium current (K_{Na}). We
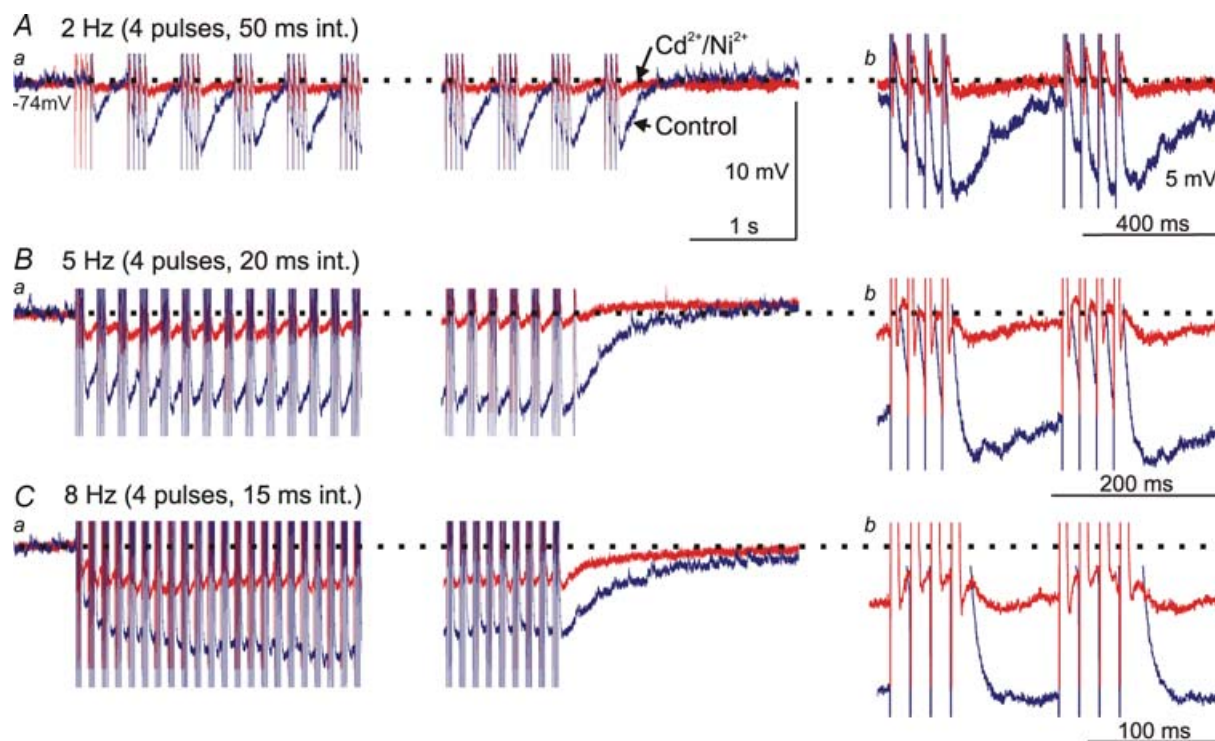

Figure 8. Summation of the sAHP during burst firing
A, bursts of action potentials were elicited by pulse train stimulation with 4 pulses (2 ms duration; 50 ms interval) and 2 Hz repetition rate. In *a* is shown the beginning and end of a 20 s long stimulation period. The summed control sAHP (blue trace) recovers between successive bursts, while not much summation is seen of the non-K_{Ca}-sAHP (Cd^{2+}/Ni^{2+}; red trace). The traces in *b* show two bursts at an expanded time scale. Dotted horizontal line indicates the membrane potential level before onset of stimulation. *B*, corresponding recording of burst firing at 5 Hz (4 pulses at 20 ms interval). The summation of the control sAHP now results in a net hyperpolarization during the 20 s stimulation period, while the non-K_{Ca}-sAHP almost recovers between bursts, which is also seen in *b*. *C*, corresponding recording of burst firing at 8 Hz (4 pulses at 15 ms interval). The summation of the control sAHP results in a net hyperpolarization during the 20 s stimulation period, as does the summation of the non-K_{Ca}-sAHP but to a much smaller degree (also evident in *b*). *A–C* are from the same cell (motoneuron, V_m was −74 mV). Scale bars in *Aa* also apply to *Ba* and *Ca*, while voltage calibration in *Ab* also applies to *Bb* and *Cb*.

therefore analysed the effect of replacing sodium with lithium ions. Lithium ions flow through voltage-gated sodium channels almost as easily as sodium ions (Hille, 1972), and action potentials can be evoked in lithium without any marked change in threshold (see Bischoff *et al.* 1998). Lithium has, however, been reported not to activate K_{Na} currents (Safronov & Vogel, 1996; Bischoff *et al.* 1998). Accordingly, when sodium ions were replaced with lithium ions in the present study, the non-K_{Ca}-sAHP was markedly reduced in amplitude (Fig. 3). Thus, the current underlying the non-K_{Ca}-sAHP appears to be sodium dependent. Next, we could conclude that this current is most likely a potassium current (Fig. 3). The responsible potassium current was further investigated in experiments with blockers (TEA, catechol) of voltage-dependent potassium channels (Fig. 4), which, rather than blocking the sAHP, caused a marked amplitude increase. This increase was proportional to the enhanced action potential area due to spike broadening, with a concomitant increase in Na^+ entry, occurring with these blockers. The

underlying potassium current is thus different from the delayed rectifier current or the transient potassium current, which are blocked by TEA and catechol, respectively.

The remote possibility that a specific activation of the sodium–potassium pump could underlie the non-K_{Ca}-sAHP was also investigated (Fig. 5; see Thompson & Prince, 1986; Morita *et al.* 1993; Scuri *et al.* 2002). The reduction of the sAHP seen with ouabain was always accompanied by a change in reversal potential for the sAHP and in resting membrane potential, and can thus be accounted for by the change of the potassium reversal potential. Furthermore, a maintained sAHP could be readily revealed during ouabain treatment by depolarizing the cell above the reversal potential. Thus, a specific activation of the sodium–potassium pump appears not to be responsible for generating the non-K_{Ca}-sAHP in this case, and possibly not in other studies that have observed a change in AHP amplitude when applying ouabain (see Parker *et al.* 1996).
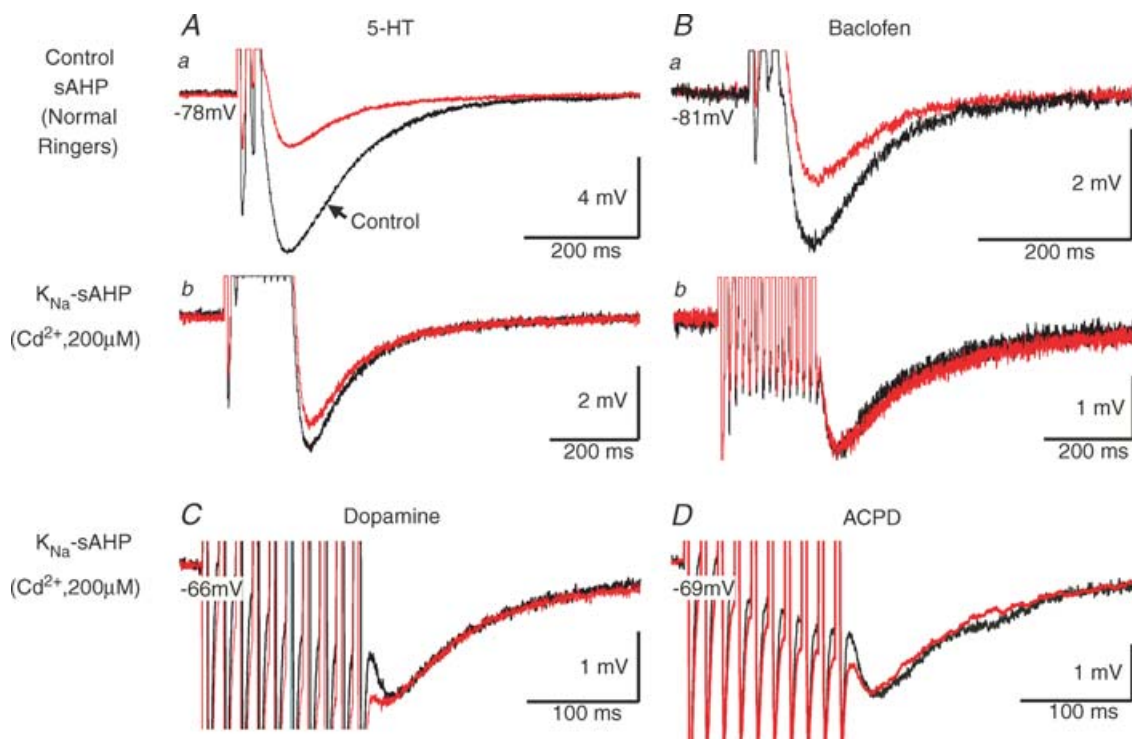

Figure 9. The non-K_{Ca}-sAHP is not influenced by 5-HT, dopamine, GABA_B or metabotropic glutamate receptor activation
A–B, test of modulatory influence of 5-HT and GABA_B receptor activation on the sAHP. During control conditions, local pressure application of 5-HT (*Aa*) or of the GABA_B receptor agonist baclofen (*Ba*) resulted in substantial reduction of the amplitude of the full sAHP (here evoked by a train of 3 spikes), as previously reported (Wallén *et al.* 1989a; Matsushima *et al.* 1993). In the presence of Cd^{2+} there was no significant effect of either 5-HT (*Ab*) or baclofen (*Bb*) on the non-K_{Ca}-sAHP (evoked by a train of 10 or 15 spikes; same grey matter neuron in *Aa* and *Ab* (V_m −78 mV) and in *Ba* and *Bb* (V_m −81 mV)). *C–D*, test of modulatory influence of dopamine and metabotropic glutamate receptor activation on the non-K_{Ca}-sAHP (evoked by a train of 10 spikes). There was no significant influence by bath application of either dopamine (*C*) or the mGluR agonist (1*S*,3*R*)-ACPD (*D*). The grey matter neuron in *C* had a V_m of −66 mV while the one in *D* had a V_m of −69 mV. In all records, black traces show the control sAHP before drug application, while red traces were taken during drug application.

All evidence thus indicates that the calcium-independent component of the sAHP is due to a sodium-dependent potassium current, a K_{Na} current. The involvement of a K_{Na} current was further corroborated in experiments using quinidine, which is reported to effectively block both cloned subtypes of K_{Na} channels (Slick (Slo2.1) and Slack (Slo2.2)) (Bhattacharjee *et al.* 2003).

The immunohistochemical data (Fig. 6) provide support for the presence of a Slack-like subtype of K_{Na} channel in the lamprey spinal cord, demonstrating distinct Slack immunoreactivity in the soma and proximal dendrites of neurons that also showed the K_{Na}-sAHP. Immunoblotting confirmed the presence of the Slack protein in the lamprey CNS. It may further be noted that the peptide region of Slack chosen to generate the antibody used here is highly conserved among multiple species (i.e. the sequence is identical in the rat, mouse, human, cow, elephant, dog, macaque and chimpanzee orthologues of the Slack channel). We also utilized the fact that the sea lamprey (*Petromyzon marinus*) genome at the moment is being sequenced, although not yet assembled. Using the sequence similarity program Discontiguous Megablast (www.ncbi.nlm.nih.gov/blast) and the rat Slack mRNA sequence (accession number AY884213) on the Whole Genome Shotgun (WGS) sequences from *Petromyzon*, we were able to pick up 18 of 32 exons (data not shown). This adds further support for the presence of a Slack-like K_{Na} channel also in lamprey.

Additional evidence for an involvement of a Slack-like subtype of K_{Na} channel is provided by the experiment with Cl^- injection. Slick is activated by both Na^+ and Cl^-, and is even more sensitive to Cl^- than to Na^+, while the Slack subtype (Yuan *et al.* 2003) shows much less Cl^- sensitivity and higher Na^+ sensitivity (Bhattacharjee *et al.* 2003). The K_{Na}-sAHP was not affected by Cl^- injection and, with these data taken together, the Slack subtype therefore appears as the most likely candidate underlying the K_{Na}-sAHP. To our knowledge, this is the first demonstration of a functional role for the Slack gene in contributing to the sAHP.

The involvement of K_{Na} currents in the generation of different types of slow afterhyperpolarizations has been described in a few other systems. A sodium-dependent sAHP seen after spike train stimulation has been reported in rat motoneurons (Safronov & Vogel, 1996), and in intrinsically bursting neurons of rat neocortex (Franceschetti *et al.* 2003). In perigeniculate neurons (ferret), spindle wave activity is followed by a long-lasting AHP, the slowest component of which (several seconds) has been suggested to rely on a sodium-dependent K^+ current (Kim & McCormick, 1998). The fact that in the present study the sodium entry during a single action potential is sufficient to activate the K_{Na} channels stands in contrast to previous reports (Dryer, 1994; Safronov & Vogel, 1996; Franceschetti *et al.* 2003), possibly indicating

close proximity between the source of sodium entry and the K_{Na} channels and/or a high sodium-affinity of the channel (see Koh *et al.* 1994; Dryer, 2003).

The fast, transient K_{Na} current occurring during the action potential (Hess *et al.* 2007) may be due to a rapid activation of K_{Na} channels in immediate proximity to the point of sodium entry, while the K_{Na}-sAHP could be generated by activation of K_{Na} channels located somewhat further away, but still close enough to allow activation upon a single spike. The difference in time course between the fast K_{Na} current during the action potential and the slower K_{Na} current underlying the K_{Na}-sAHP might then reflect the dynamics of diffusion of sodium ions along the membrane. Interestingly, the immunohistochemical analysis revealed expression of the Slack protein in both soma and dendrites of lamprey spinal neurons.

The K_{Na}-sAHP and spike frequency regulation

The sAHP is a main determinant of neuronal frequency regulation (Kernall, 1965; Schwindt & Calvin, 1973; Gustafsson, 1974; Madison & Nicoll, 1984). Lamprey spinal neurons fire repetitively in response to a prolonged depolarizing stimulus, and the interspike interval scales with the amplitude of the sAHP (Wallén *et al.* 1989*a*; Buchanan, 1993). Spike frequency adaptation may be prominent, due to the ensuing sAHP summation (Fig. 7).

In the absence of the K_{Ca}-component of the sAHP, as when blocked by a modulator, the steady state frequency was markedly increased, while spike frequency adaptation was still present, albeit less pronounced (Fig. 7). Thus, without the K_{Ca}-sAHP the cell will fire at a higher rate in response to the same excitatory input, but at the same time the presence of the K_{Na}-sAHP maintains the ability for a limited spike frequency adaptation. The K_{Na}-sAHP may therefore be viewed as a safety mechanism; in the event of a down-regulation of the K_{Ca}-component due to modulator action, the neuron will still be capable of regulating its firing behaviour.

Summation of the sAHP during rhythmic burst firing

The sAHP, with its major influence on neuronal firing properties, also plays a key role in the operation of a burst-generating neuronal network like the lamprey locomotor CPG (see Grillner *et al.* 2001; Grillner, 2003). To explore the summation effects of the sAHP during burst firing, this was simulated by repetitive stimulation with pulse trains (Fig. 8). The control sAHP recovered back to baseline between trains at the low burst rate tested (2 Hz), but at higher rates the prominent summation of the sAHP resulted in a net hyperpolarization during the period of stimulation and a slow recovery after its termination. With only the K_{Na}-component of the sAHP operating, summation became significant at higher burst rates (8 Hz),

and the net hyperpolarization was less pronounced. The K_{Na}-sAHP might thus be of particular significance during repetitive firing at higher frequencies, as will occur during faster rates of locomotor activity, even though the neuron may fire only a few spikes during the short burst.

Differential modulation of the sAHP

With the sAHP in lamprey spinal neurons being the target for several different modulatory systems, intrinsic to the spinal cord (5-HT/dopamine, $GABA_B$), it was of interest to investigate whether the action of these systems is restricted to an influence on the K_{Ca} component via their blocking effect on calcium entry (Matsushima *et al.* 1993; Schotland *et al.* 1995; Hill *et al.* 2003), or if the K_{Na} component is also subject to modulation. Neither 5-HT, nor dopamine nor $GABA_B$ receptor activation resulted in any reduction of the K_{Na}-sAHP (Fig. 9), nor did metabotropic glutamate receptor activation. The K_{Na}-component therefore may constitute a robust baseline mechanism, providing the neuron with basic membrane properties for the regulation of firing behaviour, and which is not affected by these modulators that play an important role in the spinal networks.

Implications for the operation of the spinal locomotor CPG

Several modulatory systems of the lamprey spinal cord (5-HT/dopamine, GABA, mGluR) are active during locomotor network activity, and they can thus be regarded as an integral part of the network (see Grillner, 2003). This implies that, for instance, the 5-HT system would act to reduce the K_{Ca}-component of the sAHP during network activity, causing less AHP summation and prolonged bursts and thereby contributing to the maintenance of a slow, regular burst rhythm (see Wallén *et al.* 1989*a*,*b*; El Manira *et al.* 1994). During stronger network drive and faster rhythmic activity, with shorter bursts of higher spike frequency, the K_{Na}-sAHP may become more important and even dominant, particularly if the K_{Ca} component is reduced by modulatory action. The K_{Na}-sAHP could then again be viewed as a potential safety mechanism, assuring adequate frequency regulation also when the K_{Ca} component is small.

References

Bhattacharjee A, Joiner WJ, Wu M, Yang Y, Sigworth FJ & Kaczmarek LK (2003). Slick (Slo2.1), a rapidly-gating sodium-activated potassium channel inhibited by ATP. *J Neurosci* **23**, 11681–11691.

Bhattacharjee A & Kaczmarek LK (2005). For K^+ channels, Na^+ is the new Ca^{2+}. *Trends Neurosci* **28**, 422–428.

Bhattacharjee A, von Hehn CAA, Mei X, Joiner WJ & Kaczmarek LK (2005). Localization of the Na^+-activated K^+ channel slick in the rat central nervous system. *J Comp Neurol* **484**, 80–92.

Bischoff U, Vogel W & Safronov BV (1998). Na^+-activated K^+ channels in small dorsal root ganglion neurones of rat. *J Physiol* **510**, 743–754.

Buchanan JT (1993). Electrophysiological properties of identified classes of lamprey spinal neurons. *J Neurophysiol* **70**, 2313–2325.

Cangiano L, Wallén P & Grillner S (2002). Role of apamin-sensitive K_{Ca} channels for reticulospinal synaptic transmission to motoneuron and for the afterhyperpolarization. *J Neurophysiol* **88**, 289–299.

Dale N (1993). A large, sustained Na^+- and voltage-dependent K^+ current in spinal neurons of the frog embryo. *J Physiol* **462**, 349–372.

Dryer SE (1994). Na^+-activated K^+ channels: a new family of large-conductance ion channels. *Trends Neurosci* **17**, 155–160.

Dryer SE (2003). Molecular identification of the Na^+-activated K^+ channel. *Neuron* **37**, 727–728.

El Manira A, Tegnér J & Grillner S (1994). Calcium-dependent potassium channels play a critical role for burst termination in the locomotor network in lamprey. *J Neurophysiol* **72**, 1852–1861.

Franceschetti S, Lavazza T, Curia G, Aracri P, Panzica F, Sancini G, Avanzini G & Magistretti J (2003). Na^+-activated K^+ current contributes to postexcitatory hyperpolarization in neocortical intrinsically bursting neurons. *J Neurophysiol* **89**, 2101–2111.

Grillner S (2003). The motor infrastructure: From ion channels to neuronal networks. *Nat Rev Neurosci* **4**, 573–586.

Grillner S, Wallén P, Hill R, Cangiano L & El Manira A (2001). Ion channels of importance for the locomotor pattern generation in the lamprey brainstem–spinal cord. *J Physiol* **533**, 23–30.

Gustafsson B (1974). Afterhyperpolarization and the control of repetitive firing in spinal neurones of the cat. *Acta Physiol Scand Suppl* **416**, 1–47.

Hess D & El Manira A (2001). Characterization of a high-voltage-activated I_A current with a role in spike timing and locomotor pattern generation. *Proc Natl Acad Sci U S A* **98**, 5276–5281.

Hess D, Nanou E & El Manira A (2007). Characterization of Na^+-activated K^+ currents in larval lamprey spinal cord neurons. *J Neurophysiol* **97**, 3484–3493.

Hill RH, Århem P & Grillner S (1985). Ionic mechanisms of 3 types of functionally different neurons in the lamprey spinal cord. *Brain Res* **358**, 40–52.

Hill R, Matsushima T, Schotland J & Grillner S (1992). Apamin blocks the slow AHP in lamprey and delays termination of locomotor bursts. *Neuroreport* **3**, 943–945.

Hill RH, Svensson E, Dewael Y & Grillner S (2003). 5-HT inhibits N-type but not L-type Ca^{2+} channels via $5-HT_{1A}$ receptors in lamprey spinal neurons. *Eur J Neurosci* **18**, 2919–2924.

Hille B (1972). The permeability of the sodium channel to metal cations in myelinated nerve. *J Gen Physiol* **59**, 637–658.

Kernell D (1965). The limits of firing frequency in cat lumbosacral motoneurons possessing different time course of afterhyperpolarization. *Acta Physiol Scand* **65**, 87–100.

Kettunen P, Hess D & El Manira A (2003). mGluR1, but not mGluR5, mediates depolarization of spinal cord neurons by blocking a leak current. *J Neurophysiol* **90**, 2341–2348.

Kettunen P, Krieger P, Hess D & El Manira A (2002). Signaling mechanisms of metabotropic glutamate receptor 5 subtype and its endogenous role in a locomotor network. *J Neurosci* **22**, 1868–1873.

Kim U & McCormick DA (1998). Functional and ionic properties of a slow afterhyperpolarization in ferret perigeniculate neurons in vitro. *J Neurophysiol* **80**, 1222–1235.

Koh DS, Jonas P & Vogel W (1994). Na^+-activated K^+ channels localized in the nodal region of myelinated axons of *Xenopus*. *J Physiol* **479**, 183–197.

Krieger P, El Manira A & Grillner S (1996). Activation of pharmacologically distinct metabotropic glutamate receptors depresses reticulospinal-evoked monosynaptic EPSPs in the lamprey spinal cord. *J Neurophysiol* **76**, 3834–3841.

Krieger P, Hellgren-Kotaleski J, Kettunen P & El Manira A (2000). Interaction between metabotropic and ionotropic glutamate receptors regulates neuronal network activity. *J Neurosci* **20**, 5382–5391.

Lamotte d'Incamps B, Hess D & El Manira A (2004). Control of the temporal fidelity of synaptic transmission by a presynaptic high voltage-activated transient K^+ current. *Eur J Neurosci* **19**, 3202–3210.

Madison DV & Nicoll RA (1984). Control of the repetitive discharge of rat CA 1 pyramidal neurones in vitro. *J Physiol* **354**, 319–331.

Martin MM (2002). Changes in electrophysiological properties of lamprey spinal motoneurons during fictive swimming. *J Neurophysiol* **88**, 2463–2476.

Matsushima T, Tegnér J, Hill RH & Grillner S (1993). $GABA_B$ receptor activation causes a depression of low- and high-voltage-activated Ca^{2+} currents, postinhibitory rebound, and postspike afterhyperpolarization in lamprey neurons. *J Neurophysiol* **70**, 2606–2619.

Meer DP & Buchanan JT (1992). Apamin reduces the late afterhyperpolarization of lamprey spinal neurons, with little effect on fictive swimming. *Neurosci Lett* **143**, 1–4.

Morita K, David G, Barrett JN & Barrett EF (1993). Posttetanic hyperpolarization produced by electrogenic Na^+-K^+ pump in lizard axons impaled near their motor terminals. *J Neurophysiol* **70**, 1874–1884.

Parker D, Hill R & Grillner S (1996). Electrogenic pump and a Ca^{2+}- dependent K^+ conductance contribute to a posttetanic hyperpolarization in lamprey sensory neurons. *J Neurophysiol* **76**, 540–553.

Safronov BV & Vogel W (1996). Properties and functions of Na^+-activated K^+ channels in the soma of rat motoneurones. *J Physiol* **497**, 727–734.

Sah P & Davies P (2000). Calcium-activated potassium currents in mammalian neurons. *Clin Exp Pharmacol Physiol* **27**, 657–663.

Sah P & Faber ES (2002). Channels underlying neuronal calcium-activated potassium currents. *Prog Neurobiol* **66**, 345–353.

Schotland J, Shupliakov O, Wikström M, Brodin L, Srinivasan M, You ZB, Herrera-Marschitz M, Zhang W, Hökfelt T & Grillner S (1995). Control of lamprey locomotor neurons by colocalized monoamine transmitters. *Nature* **374**, 266–268.

Schwindt PC & Calvin WH (1973). Nature of conductances underlying rhythmic firing in cat spinal motoneurons. *J Neurophysiol* **36**, 955–973.

Scuri R, Mozzachiodi R & Brunelli M (2002). Activity-dependent increase of the AHP amplitude in T sensory neurons of the leech. *J Neurophysiol* **88**, 2490–2500.

Tegnér J, Matsushima T, El Manira A & Grillner S (1993). The spinal GABA system modulates burst frequency and intersegmental coordination in the lamprey: differential effects of $GABA_A$ and $GABA_B$ receptors. *J Neurophysiol* **69**, 647–657.

Thompson SM & Prince DA (1986). Activation of electrogenic sodium pump in hippocampal CA1 neurons following glutamate-induced depolarization. *J Neurophysiol* **56**, 507–522.

Uchino S, Wada H, Honda S, Hirasawa T, Yanai S, Nakamura Y, Ondo Y & Kohsaka S (2003). Slo2 sodium-activated K^+ channels bind to the PDZ domain of PSD-95. *Biochem Biophys Res Commun* **310**, 1140–1147.

Wallén P, Buchanan JT, Grillner S, Hill RH, Christenson J & Hökfelt T(1989*a*). Effects of 5-hydroxytryptamine on the afterhyperpolarization, spike frequency regulation, and oscillatory membrane properties in lamprey spinal cord neurons. *J Neurophysiol* **61**, 759–768.

Wallén P, Christenson J, Brodin L, Hill R, Lansner A & Grillner S(1989*b*). Mechanisms underlying the serotonergic modulation of the spinal circuitry for locomotion in lamprey. *Prog Brain Res* **80**, 321–327.

Wallén P & Grillner S (2003). One component of the slow afterhyperpolarization in lamprey neurons is mediated by a Na^+ activated K^+ current. *Soc Neurosci Abs* 53.52.

Wallén P, Hess D, El Manira A & Grillner S (2002). A slow non Ca^{2+} dependent afterhyperpolarization in lamprey neurons. *Soc Neurosci Abs* 546.549.

Wallén P, Robertson B, Bhattacharjee A, Kaczmarek LK & Grillner S (2005). K_{Na} channels of the Slack subtype underlie the non-Ca component of the slow AHP in lamprey spinal neurons. *Soc Neurosci Abs* 152.155.

Wikström MA & El Manira A (1998). Calcium influx through N- and P/Q-type channels activate apamin-sensitive calcium-dependent potassium channels generating the late afterhyperpolarization in lamprey spinal neurons. *Eur J Neurosci* **10**, 1528–1532.

Yuan A, Santi CM, Wei A, Wang ZW, Pollak K, Nonet M, Kaczmarek L, Crowder CM & Salkoff L (2003). The sodium-activated potassium channel is encoded by a member of the Slo gene family. *Neuron* **37**, 765–773.